Chapter 4: Generation and Evaluation of a Large Mutational Library from the *E. coli* Mechanosensitive Channel of Large Conductance, MscL. Implications for Channel Gating and Evolutionary Design.

4.1 Introduction

Since its cloning in 1994 by the Kung labs (Sukharev et al., 1994), the mechanosensitive channel of large conductance (MscL) has developed into a prototype ion channel for understanding cellular mechanosensation (Blount and Moe, 1999; Hamill and Martinac, 2001; Sukharev et al., 1997; Wood, 1999). Much of what is known about the function of MscL has been gained through investigation of the *E. coli* channel using electrophysiology and mutagenesis (Blount and Moe, 1999; Hamill and Martinac, 2001; Sukharev et al., 1997). Electrophysiological characterization of Ec-MscL in both bacterial spheroplasts and reconstituted lipid vesicles has: demonstrated that MscL is opened by tension from the lipid bilayer (Sukharev et al., 1994); quantitated the tension required to open MscL (Sukharev et al., 1999); predicted the pore size of the open channel (Cruickshank et al., 1997); and suggested that there are several discrete steps on the opening pathway (Sukharev et al., 1999). Mutagenesis studies also determined that the first transmembrane region of Ec-MscL lined the pore and established an occlusion of the channel in the vicinity of residue G22 (Blount et al., 1997; Blount et al., 1996; Ou et al., 1998) (Yoshimura et al., 1999).

A breakthrough in the study of MscL came with the report from the Rees labs of the high resolution crystal structure of MscL from *M. tuberculosis* (Tb-MscL) (Chang et al., 1998). This result confirmed many of the essential conclusions of the earlier mutagenesis studies, while also clarifying some confusion concerning the stoichiometry of the channel and providing a wealth of new insights into the molecular details of the structure.

The image of Tb-MscL produced by Rees and coworkers is undoubtedly of the closed state of the channel. Of the many challenges associated with the detailed study of channels and other membrane proteins, a major issue is the elucidation of the several states–open, closed, intermediate, desensitized–associated with such structures and the mechanisms of the transitions among them. For a type of bacterial K^+ channel images of the open and closed state are now available (Doyle et al., 1998; Jiang et al., 2002; Zhou et al., 2001), but this is not the case for MscL nor other channels. As such, other approaches to analyzing the open state of the channel have been employed.

Interesting results have been obtained from molecular dynamics simulations beginning from the closed state of MscL (Elmore and Dougherty, 2001; Gullingsrud et al., 2001; Kong et al., 2002). At present, however, it is not possible to run such simulations long enough to see the transition from closed to open state. As a result, the de novo construction of molecular models for the open state and various intermediates on the opening pathway has been attempted.

In particular, a detailed, atomic-level gating model for Ec-MscL has been developed by Sukharev, Guy, and co-workers (SG) (Sukharev et al., 2001a; Sukharev et al., 2001b). Although the Rees crystal structure is of Tb-MscL, SG chose to model Ec-MscL so that use could be made of the much larger collection of experimental data that exists for this homologue. These data were used extensively in developing the computational model. In addition to emphasizing key residues identified from the mutagenesis studies, the SG model naturally identified a number of other key interactions that make important

contributions in the open state and in a key intermediate state identified along the gating pathway. Recently, spin labeling studies from the Perozo lab have provided some support for the global structural model of the transmembrane domains developed by SG (Perozo et al., 2002a).

In order to test specific features of the SG model, it would be useful to evaluate the many proposed structural contacts by site-directed mutagenesis. However, the protocols for evaluating MscL mutants–either electrophysiology or growth studies–are time-consuming and tedious. Also, two distinct MscL mutant phenotypes have been identified using electrophysiology: gain of function mutations (GOF), which are mutations that open spontaneously or with less tension than required to open wild type MscL; and loss of function mutations (LOF), which are mutations that can not be gated or require more tension than wild type MscL to gate. Previous mutagenic studies, however, have almost exclusively evaluated GOF mutations only, as the LOF assay is especially tedious.

Recently, we have developed a high-throughput, fluorescence-based method for the phenotypical characterization of both LOF and GOF mutations in Ec-MscL (Maurer and Dougherty, 2001). This approach allows for the rapid screening and identification of mutations that are phenotypically wild type, gain of function, or loss of function. We now report the results of an extensive random mutagenesis study of Ec-MscL, looking at mutations with both possible phenotypes. We have greatly expanded the number of MscL mutants with an altered phenotype, especially for the LOF phenotype. These mutagensis results have been used to evaluate several key features of the SG gating

model. In addition, our mutagenesis results implicate particular regions of MscL as being involved in tension sensing and may discriminate between two proposed evolutionary models of MscL.

4.2 Results

4.2.1 The Library

A library of random mutations was created using a standard sloppy PCR protocol, as described in the Methods section. Starting with this library, 408 Ec-MscL constructs were sequenced and phenotypically screened. The resulting constructs had a modal distribution centered at 2-3 nucleotide changes per construct and one amino acid change per construct. The distribution of mutations is shown in Figure 4.1. Of the 408 sequenced constructs, 348 contained at least one amino acid change in the MscL protein.

Of the constructs that contained at least one amino acid point mutation, 64% were phenotypically wild type, 29% were phenotypically loss of function, and 7% were phenotypically gain of function. Looking only at the constructs with a single amino acid change, 74% were wild type, 20% were loss of function, and 6% were gain of function. These results are in striking contrast to previous work, which has primarily identified gain of function mutations.

As expected, increasing the number of mutations increased the probability of a channel showing an altered phenotype (GOF or LOF). Figure 4.2 shows the number of occurrences of a particular phenotype as a function of the number of amino acid point

mutations. The large number of phenotypically wild type mutations observed, coupled with the observation of phenotypically wild type constructs that contain multiple mutations (up to 7), suggests that MscL is relatively tolerant to mutation.

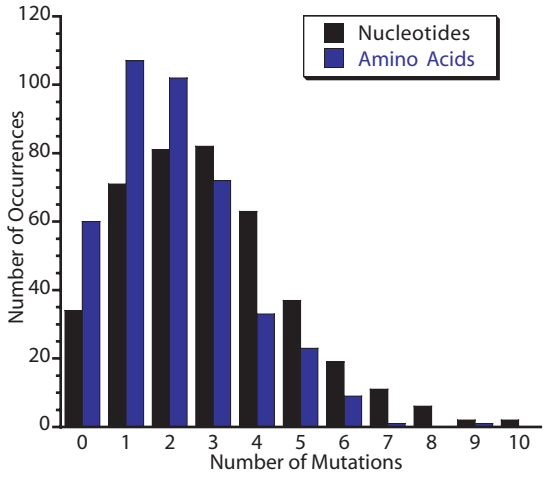

Figure 4.1: Distribution of nucleotide and amino acid mutations observed in the library of 408 sequenced Ec-MscL constructs.

Ninety percent of the amino acids that make up Ec-MscL were mutated at least once in our sequenced random mutation library. A modal distribution centered around 3 amino acid changes per Ec-MscL residue was observed (Figure 4.3). Up to seven different amino acids changes were observed at a single Ec-MscL position. Assuming a single nucleotide change per codon in Ec-MscL, there are 843 possible non-silent point mutations. Forty-six percent (390) of all possible point mutations were observed in our sequenced random mutation library.

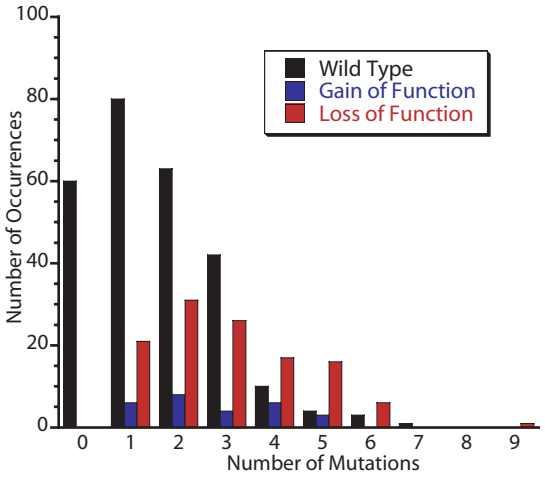

Figure 4.2: Phenotypic distribution of sequenced Ec-MscL constructs.

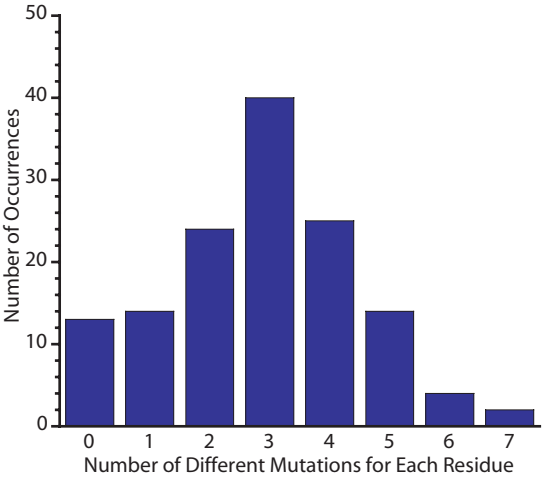

Figure 4.3: Distribution of the number of amino acid mutations observed for a given residue in Ec-MscL.

4.2.2 Evaluating Multiple Mutations

Single-site mutants are, of course, straightforward to interpret, whether they give wild type, GOF, or LOF phenotypes. On the other hand, interpreting the results for structures with multiple mutations can be challenging. If we assume that the occurrence of compensating LOF and GOF mutations is rare, multiple mutations that are phenotypically wild type arise from a collection of phenotypically wild type mutations. To test this assumption we can use the number of single-site, wild type mutations to predict the expected number of multi-site wild type mutations. That is, if 75% of single-site mutants are wild type, then we expect the fraction of double mutants that are wild type to be $(0.75)^2$. The predicted and actual fractions of wild type phenotypes for multiple mutants are shown in Figure 4.4, and the agreement is acceptable. We therefore assume that a mutation that occurs in any wild type construct is a "wild type" mutation and would produce a wild type phenotype if it occurred as a single mutant. This also means that such a mutation does not contribute to GOF or LOF phenotypes.

Constructs with multiple mutations and an altered phenotype are more difficult to interpret, since any single mutation could give rise to the observed phenotype. Pseudo-single-site, altered phenotype mutation data can be generated, however, by subtracting the wild type data from the non-wild type data. In this process, if the same mutation is observed in both a wild type construct and an altered phenotype construct, the mutation is assumed not to give rise to the altered phenotype. For example, the double mutant V23A/K117T is observed to be gain of function, and the mutation K117T is observed in a wild type construct. From this we conclude that the mutation V23A gives rise to the

observed gain of function phenotype. Additional pseudo-single-site data can be obtained by assuming that mutations to Ec-MscL beyond residue 110 are wild type. It has been shown that deletion of residues 110-136 in Ec-MscL does not dramatically alter the gating of the channel.

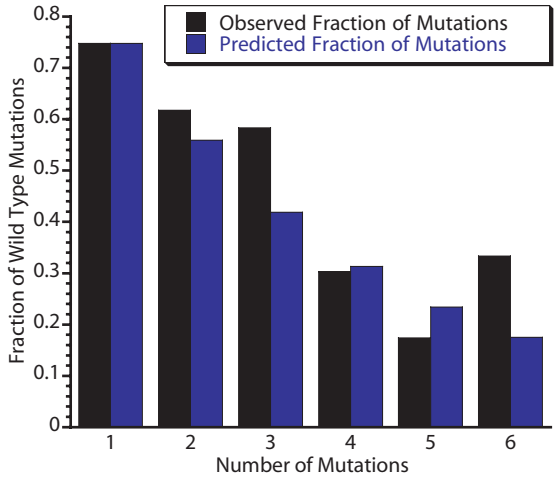

Figure 4.4: Comparisons of the observed number of phenotypically wild type mutations with the predicted number of phenotypically wild type mutations.

Similar to the analysis of wild type mutations, the number of LOF and GOF mutations can be predicted from the number of single-site mutations, using the assumption that one mutation gives rise to a particular phenotype. The number of observed mutations is again similar to the predicted value (data not shown).

The single-site and pseudo-single-site mutations that produce altered phenotypes are shown mapped onto the SG closed state structure in Figure 4.5, and the data are collected in Tables 1 and 2. Interestingly, the phenotypically altered single-site data suggest that

TM2 is functionally significant. Two new gain of function mutations are observed in this region, F83Y and L86Y, along with many loss of function mutations. With the exception of N100D, mutations in TM2 with altered phenotypes had not been observed in previous random screenings of Ec-MscL.

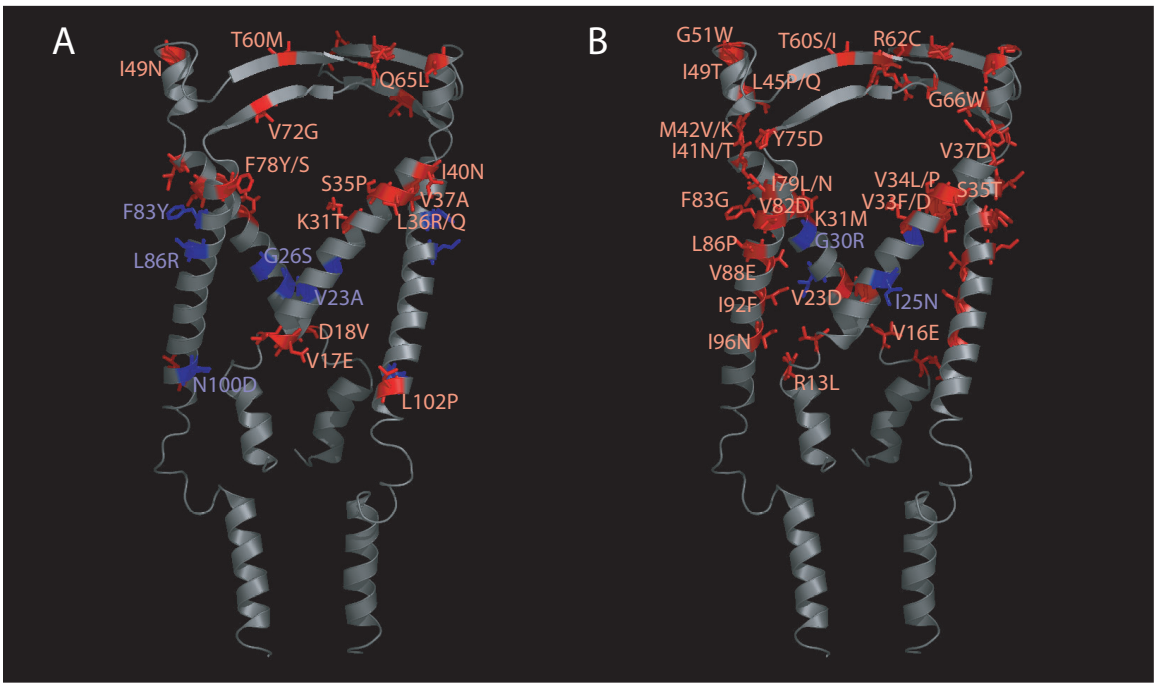

Figure 4.5: Phenotypically non-wild type mutations mapped onto the SG closed state structure. Loss of function mutations are shown in red and gain of function mutations are shown in blue. (A) Observed single-site mutations. (B) Observed pseudo-single-site mutations.

Previous work had identified roughly 30 gain of function mutations in Ec-MscL, and the 7 GOF constructs observed here add 5 new entries to that list. In contrast, previous work had identified only 10 loss of function mutants, and so the discovery of 45 new LOF mutants greatly expands the list and has significant implications for channel function and design, as discussed below. Additionally the 237 single-site wild type mutations or

pseudo-single-site wild type mutations provide additional information that was not previously available.

4.3 Discussion

Using a standard sloppy PCR protocol and a recently developed high-throughput screen, we have been able to evaluate 408 Ec-MscL constructs, of which 348 contained at least one altered amino acid. The coverage of mutations is good and fairly uniform (Figure 3a). We feel the results have significant implications for several aspects of MscL research, including the details of the SG model, possible tension-sensing regions, and some recent speculations on the evolutionary origin of MscL.

An important contribution from these studies has been the discovery of 45 new LOF mutations. Prior to this work, only 10 LOF mutants were known, all of which were variants at the G22 site that also produces GOF mutants.(Yoshimura et al., 1999) Previous studies have primarily focused on GOF mutants, no doubt because of the greater challenge in performing conventional LOF assays. The conventional LOF assay is not amenable to high-throughput screening, therefore all previously identified LOF mutations were discovered using electrophysiology. The fluorescence assay used here overcomes this problem and provides a different perspective on the relative likelihood of GOF vs. LOF mutations. Using this assay 29% of the constructs containing one or more mutations were LOF and 20% of all constructs containing precisely one mutation were LOF (Figure 1b). In sharp contrast, only 7% of all constructs containing at least one mutation were gain of function and only 6% of constructs with precisely one mutation

were GOF (Figure 1b). Of the single-site plus pseudo-single-site mutations 82% were wild type, 16% were LOF and 2% were GOF. The percentage of these mutations that are wild type is slightly higher than when considering all mutations because many of the multi-site LOF and GOF mutations could not be resolved to pseudo-single-site mutations.

4.3.1 Implications for the SG Model

The starting point for the SG model is a modified homology model of the Tb-MscL crystal structure of the closed state. A new helix (S1, see Figure 4.6) was added to the amino terminus of the protein, corresponding to a region that was not resolved in the Tb-MscL crystal structure. Also, since the loop region of MscL is not well conserved between the *E. coli* and the *M. tuberculosis* homologues, a de novo model for the Ec-MscL loop region, not based on the crystal structure of Tb-MscL, was developed. Additionally, the carboxyl terminus of the protein was adjusted to make room for the S1 region. The various regions of the model are shown in Figure 4.6a.

A key feature of the SG model is the presence of an expanded, intermediate state on the gating pathway. In this state the occlusion of the pore seen in the crystal structure is broken, but an occlusion formed by the modeled S1 helices remains. This pre-expanded state was considered necessary to explain the electrophysiology of Ec-MscL. Figure 4.6b, 1.6c, and 1.6d show a top view of the SG model for the closed, expanded intermediate, and open states, respectively.

Table 1 – Conserved Residues in the SG Model

Wild Type Residue	Closed State Interactions	Pre-expanded State Interactions	Open State Interactions	Observed Wild Type Mutations	Observed Gain of Function Mutations	Observed Loss of Function Mutations
S1 Helix						
E6	F7, R8	F7, R8, K130	G22, I25, G26	D		
F7	I3, E6, F7, F10	I3, E6, F7, F10	A89, I92, F93, I96, L129	S, C, L		
R8	E6, E107	E6, D127, K130, E131, Q132	R126, D127, L129, K130, E131			
E9	A11, R13, K106	All, R13, R126, K130	R126, K130	T, G		
F10	F7, F10, N15, D18, L19	F7, F10, All, R13	G14, I25, A28, F29, I32, F85, A89, I92	L, I		
All	E9, R13, N15	E9, F10, R13	I125, R126, L129	V		
R13	E9, A11, G14, N15, V17, D18, N100	E9, F10, A11, D18, L19, I25	D18			L
G14	E9, R13, V16, D18	E9, L19, I25, L122, I125, R126	F10, F29			
First Transmembrane Domain (TM1)						
N15	E9, F10, R13, D18	D18, L122, E118, E119, R126		S, Y, K		
V16	G14, D18, V21, G22, I96	F29, F85, L122, E119	L36, F78	M, A		E
V17	R13, G22, I96, I99	I96, I99, L129	I32, I40	A		E
D18	F10, R13, G14, N15, V16, L19	R13, N15, R126, L129, K117	R13	E		V
L19	F10, L19, D18	R13, G14, I25, F29, F85	G14, F29, V33			
A20	G22, G26, I25	F29	V33, L36, V37, I40	V		
V21	I92, I96	I92, I125, L128, L129	I3, I40, I92			
G22	V17, L19, A20	M12, L129	M1. I3. E6			
V23	V23, G26	F29, G30, V33,	M1, V33, V37	I	A	D
I24	G26, F29, I92, V88	V33, L36, V37, V88, I92	V37, I40, I41, P44	V, T	N	
I25	A20, F85, V88, A89, I92, F93	R13, L19, F85, V88, I92, I125	I3, E6, F7, F10, I92		S	
G26	A20, V23, I24	R13	E6			
A28	F85, V88	V37, V88	F10, F85, V88			
F29	I24, F85, I87, V88, A91	V16, L19, A20, V23, F85	F10, G14, L19	S, V, Y		
K31	S34, Q80, N81, D84	I41, Q80, N81, D84	Q80, N81, D84	R		T
I32	N81, F85	N81, F85	F10, V16, N81, F85	T, V		
V33	D84, I87, V88	V23, I24, A27	L19, A20, V23	A, S. I		F, D
L36	F78, N81	I24, F78, N81	V16, A20, F78, N81	P		R, Q
V37	Q80, F83, D84, I87	I24, A27, A28	A20, V23, I24			A, D
I40	M42, F78	F78, I87, V88	V16, V17, A20, V21, I24			N
Periplasmic Loop (Loop)						
M42	D39, I40, I45	M73	V71, V72, M73	G, T, I		V, K
P43	F54					
P44	F54, K55, I68. Y75	Q80	I24			
L45	M42, I68, V71, V72	V71, V72, M73	P69, A79, V71			P, Q
G51		A64, L61	Q80, F83	V, E, R		W
D53	I47, Q65	I47, K55, Y75	G76, Q80	N, E, G		
F54	P43, P44, Y75	I47, Y75	Y75, G76, I79	S, L		
Second Transmembrane Domain (TM2)						
Y75	P44, F54, I41	F54, K55, D53	F54, K55, Q56	C		D
G76			D53, F54	S		
F78	L36, D39, I40	L36, D39, I40	V16, L36	L, I		Y, S
I79			I52, F54	V		L, N
F85	I25, A28, F29, I32	V16, L19, I25, A28, F29	F10, I32	L		
I87	F29, I33, V37	I40	I47	T, V, F		
A89	I25	L121, L122, I125	F7			
A91	F29			T		
I92	V21, I24, I25	V21, I24, I25, I125	I3, F7, F10, V21, I25	T, V, L		F
F93	I25	L121, E124, I125	F7, L129	L, S		
I96	R13, V16, V17, V21	E124, I125, L128	I3, I4, F7	V, M		N
K97		E124	Q132	E, R		
N100	R13	R104, E108, A111, P113	Q132, N133	Y, S	D	
C-terminal Helix (C-Helix)						
L121	L121, L122, I125	A89, F93	M12	E, I, S		
L122	K117, V120, L121, E124	G14, N15, V16, F85, A89	M12, R13	P, Q, R		
E124	L122, I125, R126	F93, K97		G, D, K		
I125	I121, I125, E124, L128	G14, V21, I25, I92, F93, I96	A11, M12	R, N, F, V, T		
R126	E124, D127	E9, N15, D18, E118	R8, E9, D127	P, H		
D127	R126, L129	R8	R8, R126	V, G		
L128	L128, L129	V17, V21, I96, P113		S, M		
L129	D127, L128	M12, R13, D18, V21, G22	F7, R8, A11, F93	P, Q, R		

Table 2 – Non-Conserved Residues in the SG Model

Wild Type Residue	Observed Wild Type Mutations	Observed Gain of Function Mutations	Observed Loss of Function Mutations
S1 Helix			
S2	L, G, N		
I3	F, N , T, V		
I4	N, T		
K5	N, Q, R		
M12	K, L, R, T, V		
First Transmembrane Domain (TM1)			
A27	V		
G30		R	
S34	T		L, P
S35			P, T
A38	T		
D39	E, N, V		
I41	V		N, T
Loop			
G46			
L47	F		
L48	F, I, S		
I49	F, V		N, T
G50			
I52	N, V		
K55	E, I, N, R		
Q56	L. R		
F57	I, L, S, V		
A58	T		
V59	A, I		
T60	A, E, K		M, S, I
L61			
R62	L		C
D63	G, V		
A64	E, S		
Q65	R		L
G66	V		W
D67	E, G		
I68			
P69			
A70			
V71	A, I		
V72	A, I		G
M73	K, L, T, V		
H74	L, Q, R,		
Second Transmembrane Domain (TM2)			
V77	A, D		
Q80	R		
N81	D, I, S		
V82	A, P		D
F83	I, L, S	Y	G
D84	E, G, V		
L86		R	P
V88	G, L		E
F90	C, L, S, V		
M94	I, L, T, V		
A95	V		
L98			
I99	N, T		
TM2 – C-Helix Linker (Linker)			
K101	E, N, Q, R		
L102	E, Q		P
N103	D, H, K, S		
R104	W		
K105	E, N		
K106	E, R		
E107	K, V		
E108	D, G, K		
P109			
A110	T		
A111			
A112			
P113			
A114	V		
P115	Q, S		
T116	A, S		
K117	R, N		
E118	D, G, Q, V		
E119	A, D, G		
C-terminal Helix (C-Helix)			
V120	A		
T123	A, S		
K130	E, N		
E131	G		
Q132	R, P, V		
N133	D, H, I, S, Y		
N134	D, E, I, S, T		
R135	C		
S136	P, T		

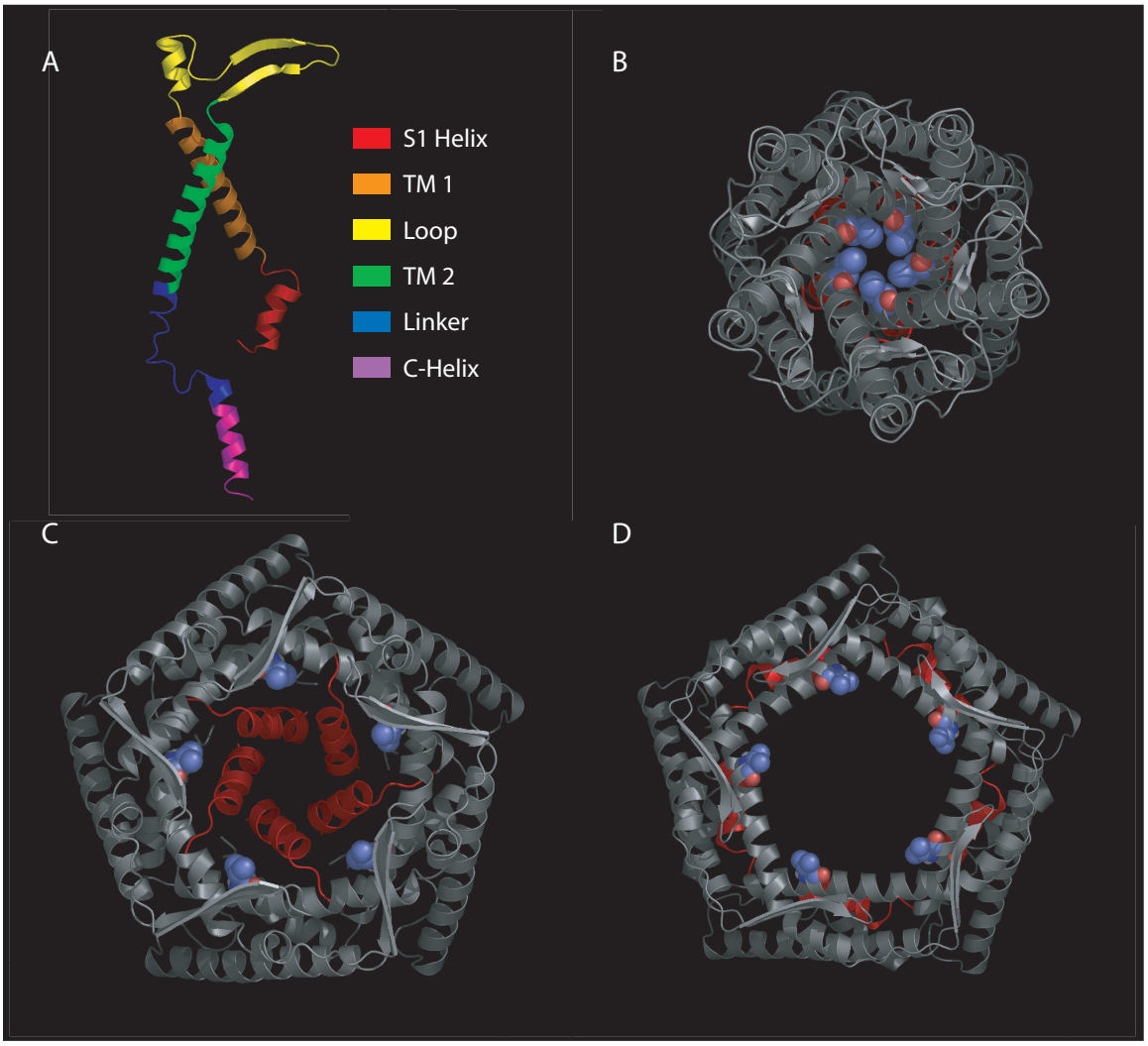

Figure 4.6: (A) A single chain of the SG closed state model highlighting the various regions of the protein. (B-D) Top views of the SG closed state model, intermediate state model, and open state model with the V23 plug shown in CPK and the putative S1 helix shown in red.

In the present work, we use specific point mutations to probe features of the SG model. It is difficult for a study of point mutations to provide compelling evidence in support of or opposed to the global structural changes inherent in the SG model, and we note that the global model for the first and second transmembrane domains has received some experimental support (Perozo et al., 2002a). Still, evaluating particular amino acids is justified by the fact that the SG model was created with a strong reliance on the

assumption that highly conserved residues are important and should be involved in complementary interactions in the closed, pre-expanded, and/or open states (Sukharev et al., 2001b). Relying on sequence conservation is inherently challenging for MscL, because conservation across the family is not nearly as extensive as is typical for homologous proteins. Also, a detailed sequence analysis from our labs (Maurer et al., 2000) produced two distinct MscL subtypes, with Tb-MscL, the sequence for which a crystal structure exists, lying in a different family from Ec-MscL, the sequence modeled by SG.

Table 1 shows the proposed interacting partners for the conserved residues in each state based on the SG model, and the mutations we have observed for these residues. It is clear from this table that many of the residues postulated to be involved in key interactions in the various states of the model can be mutated and yet still produce a wild type phenotype. This calls into question the degree to which a given interaction is essential for proper channel function. Furthermore, no direct correlation is observed between sequence conservation and mutational tolerance for a given residue. As can be seen from Table 1, mutations were observed for most of the conserved residues, with many producing a wild type channel. This is especially true for residues located in the amino and carboxyl termini of the protein. In the non-terminal regions of MscL, the number of sites having mutations that give rise to an altered phenotype is not appreciably different between the conserved (Table 1) and non-conserved residues (Tables 2).

Several attempts to correlate mutational tolerance with sequence conservation were made by applying the Rao physio-chem scoring matrix (Rao, 1986) to the observed mutational data and our sequence alignment. However, in no case was a correlation between mutational tolerance and sequence alignment observed (data not shown). These results highlight the previously noted fact that sequence conservation among the MscL channels is not high, with some tendency for homologues to cluster into specific subtypes.

4.3.1.1 The Role of S1and the Five Conserved Phenylalanines.

The SG model makes many predictions about key interactions involved in various states of MscL. SG observe five highly conserved phenylalanines in the MscL family and assign significant functional roles to all of them. The first two, F7 and F10, are proposed to reside in the hypothetical S1 helix that is not observed in the Tb-MscL crystal structure; the third phenylalanine, F29, resides in the first transmembrane domain; and the final two phenylalanines, F85 and F93, reside in the second transmembrane domain. Our data suggest that none of these residues are critical to channel function.

The SG model postulates that in the closed state F7 and F10 interact with each other to occlude the pore and serve as a secondary gate. We observe mutagenic tolerance at F7 for serine, cysteine, and leucine and mutagenic tolerance at F10 for leucine and isoleucine. While the F10 mutations could be considered conservative, those at F7 are certainly not, arguing against a key F7•••F10 interaction. Note that Sukharev *et al.,* had previously shown, using electrophysiology, that the F7C mutant was functional in the absence of disulfide formation (Sukharev et al., 2001a).

In the pre-expanded states of the SG model, it is postulated that F10 from one subunit interacts with F7, I3, and I4 of the neighboring subunit. Mutations that have been observed to be phenotypically wild type at I3 are threonine, valine, phenylalanine, and asparagine; and at I4 threonine and asparagine give wild type behavior. The significant mutagenic tolerance at these positions is supported by the observation of Blount *et al*. that residues 2-4 of Ec-MscL can be deleted without significantly altering channel function (Blount et al., 1996). These results suggest that the blockage in the pre-expanded state of the channel, which is necessary to explain the electrophysiology of MscL, may not be due to the postulated S1 helices.

As with the closed and pre-expanded states, F7 and F10 are proposed to exert significant influence over the open state. In the open state of the channel, F7 is postulated to interact with F93, and F10 is postulated to dock between F29 and F85. Again mutagenic tolerance is observed for F29, F85 and F93. Mutations of F29 to serine, valine, and tyrosine are tolerated; mutation of F85 to leucine is tolerated; and mutations of F93 to serine and leucine are tolerated. It seems unlikely that the proposed aromatic-aromatic interactions play critical roles in the function of MscL.

While one could argue that mutational tolerance at any given site might not make a compelling case, the range of conserved residues that can in fact be mutated without phenotypical consequences suggests that the S1 helix developed for the SG model may not play a crucial role in MscL function. The lack of an important functional role for the

S1 helix is in agreement with the intermediate proposed by Perozo and co-workers (Perozo et al., 2002a), however the lack of an expanded intermediate in the Perozo model does not fit well with the electrophysiology data (Sukharev et al., 1999).

4.3.1.2 An Important Aspartic Acid.

All conformations of the SG model are proposed to be stabilized by a salt bridge between R13 and D18. Interestingly, D18E is observed to be phenotypically wild type, while D18V is observed to be phenotypically loss of function. This supports the proposed importance of an acidic residue at position 18. Unfortunately, no mutations were observed for R13.

4.3.1.3 Unimportant Salt Bridges.

Two other salt bridges were specifically noted by SG as important for stabilization of the open state: R8•••D127 and E9•••R126. Clearly these salt bridges are not necessary for gating, as E9 can be mutated to glycine and threonine; R126 can be mutated to proline and histidine; and D127 can be mutated to valine and glycine, with all mutants giving a wild type phenotype. The lack of importance of these salt bridges is further highlighted by the fact that Ec-MscL truncated at position 110 is phenotypically wild type (Blount et al., 1996; Hase et al., 1997).

4.3.2 The Tension Sensor

In an effort to gain some insight into which residues are most crucial to channel function, we have mapped onto the proposed closed state structure of Ec-MscL the distribution of single-site and pseudo-single-site loss of function mutations (Figure 4.7). We assume that LOF mutants are more likely associated with key functional regions of the protein than GOF mutants, and the discovery of a large number of new LOF mutants is thus a key feature of this work. LOF mutations are clearly concentrated in the loop region and in the regions of the protein near the headgroups of the lipid bilayer. It is striking that very few loss of function mutations are observed in the middle of the transmembrane domains and that no loss of function mutations are observed in the C-terminal region.

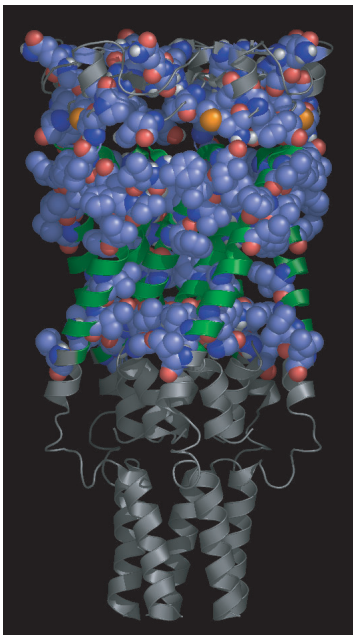

Figure 4.7: Loss of function mutations shown as CPK on the SG closed state structure.

The lipid head groups provide a means for specific protein-lipid interactions. Molecular dynamics simulations of Tb-MscL have established strong interactions between the lipid headgroups and the MscL channel (Elmore and Dougherty, 2001; Elmore and Dougherty, 2002). The same simulations have shown that the number of hydrogen bonds between the protein and the lipid varies as a function of the lipid head group.

Several lines of experimental evidence also point to a key role for lipid-protein interactions in gating mechanisms. Gating tensions for Ec-MscL in native *E. coli* membranes, which are predominately phosphatidylethanolamine, are measurably higher than gating tensions for Ec-MscL reconstituted into phosphatidylcholine (Sukharev et al., 1997), and the hydrogen bonding potentials of these two lipids are substantially different (Elmore and Dougherty, 2001; Elmore and Dougherty, 2002). Matinac and Hamill have shown that small changes in lipid chain length can greatly affect the mechanosensitive gating of gramicidin A (Martinac and Hamill, 2002). Furthermore, Perozo and Martinac have shown that reconstitution of Ec-MscL into vesicles made up of lipids with progressively shorter chain lengths results in a channel that is progressively easier to open (Kloda and Martinac, 2001; Perozo et al., 2002b). Additionally, Martinac and Hamill have argued that changes in bilayer thickness due to tension, which they estimate to be less than 1.5Å, are important for the gating of mechanosensitive channels (Hamill and Martinac, 2001; Martinac and Hamill, 2002).

Further, although less direct, support for key lipid-protein interactions, comes from the observation by Jones *et al*. that Ec-MscL gates upon heat shock (Jones et al., 2000). One

aspect of thermal adaptation for *E. coli* is a change in membrane composition, with shorter lipids being more common at higher temperatures (Bright-Gaertner and Proulx, 1972; Suutari and Laakso, 1994). In addition, significant differences in gating tensions exist between Ec-MscL and Tb-MscL, and the native lipid bilayers of *E. coli* and *M. Tuberculosis* are different (Bright-Gaertner and Proulx, 1972; Lee et al., 1996; Lugtenberg and Peters, 1976; Suutari and Laakso, 1993; Suutari and Laakso, 1994). Taken together, these experimental observations are consistent with our observation that LOF mutants are clustered near the lipid headgroups, where the interactions with the protein are the strongest.

4.3.3 The Loop

A significant number of the single-site and pseudo-single-site loss of function mutations observed for Ec-MscL are located in the loop region (Figure 4). Previous work by us and others has implicated this region as being important in MscL gating (Ajouz et al., 2000; Blount et al., 1996; Gu et al., 1998; Maurer et al., 2000). For Tb-MscL it has been shown that modification of a charged hydrogen bond in the loop results in mutations that are phenotypically gain of function. (Maurer et al., 2000) Martinac and co-works have shown that in Ec-MscL, proteolytic cleavage of the loop results in gain of function behavior for Ec-MscL (Ajouz et al., 2000). Conversely, Blount *et al*. have shown that deletion of a single residue, Q56, from the Ec-MscL loop results in a loss of function phenotype (Blount et al., 1996). This has led to the hypothesis that the loop serves as a spring connecting the first transmembrane domain and the second transmembrane

domain. The observed loss of function mutations in this region further support this hypothesis.

4.3.4 Evolutionary Arguments about Mechanosensitive Channels

Morris and co-workers have proposed two hypotheses to account for the evolution of mechanosensitive ion-channels (Gu et al., 2001; Tabarean and Morris, 2002). The first hypothesis is that mechanosensitive channels have evolved with either specialized mechanogating regions, a global structure that renders them susceptible to bilayer tension, or both. The second, less conventional, hypothesis is that mechanosensitive channels respond to bilayer tension because it has been evolutionarily impossible, undesirable, and/or unnecessary to eradicate intrinsic protein characteristics that result in mechanosensitivity. That is, mechanosensitivity is a natural feature of all membrane channels. Those channels that are not mechanosensitive, or have high tension thresholds like MscL, must have acquired special structural features to *diminish* the innate mechanosensitivity of ion channels. Morris and co-workers have argued that the second hypothesis is more compelling than the first, citing evidence that mechanosensitivity is harder to design out of a protein than to design into a protein. Their evidence for this is the mechanosensitivity of Shaker-IR and the "ample selection of MscL mutants that produce a channel more mechanosusceptible than the wild type"(i.e., GOF mutants) (Gu et al., 2001).

We assert that true mechanosensitive channels arise from the first hypothesis, and that MscL is one of these channels. Our mutational data clearly show that a mutation is much

more likely to create a *loss* of function phenotype than a gain of function. This implies that it is more difficult to design mechanosensitivity into MscL than it is to design mechanosensitivity out of MscL. As noted above, the reason that previous random mutagenesis studies of MscL did not uncover many phenotypically loss of function channels is that the screening assay used was incapable of distinguishing loss of function mutations from wild type. The hypothesis that mechanosensitivity is difficult to design into "true" mechanosensitive channels is further supported by random mutagenesis studies on MscS performed by Blount and co-workers (Okada et al., 2002). These studies show that it is extremely difficult to identify mutations that make MscS easier to gate. Additionally, our single-site and pseudo-single-site loss of function data point to a specialized mechanogating region as required by the first hypothesis. While mechanosensitivity may exist in non-mechanosensitive channels, it seems clear that "true" mechanosensitive channels have been designed to open under very specific conditions.

4.4 Conclusions

Although the general mechanism of gating proposed by SG may or may not describe the opening pathway for Ec-MscL, it seems likely that some details of the model need further refinement. Many of the highly conserved residues, which are assigned important roles in the model, can undergo dramatic mutations while preserving a phenotypically wild type channel. In particular, the putative S1 helix bundle was assigned the important role

of forming a second gate in the closed and intermediate states, but that conclusion is not supported by the data presented here.

The clustering of loss of function mutations along the lipid head groups at the top and bottom of the membrane may indicate that this region is responsible for tension sensing in MscL. Additionally, the identification of many loss of function mutations in the loop region provides further evidence that the loop serves as a transduction domain connecting the first and second transmembrane domains. In general, phenotypically altered mutations occur in the first transmembrane domain, loop, and second transmembrane domains. This argues for the importance of these regions in the gating of MscL. The putative S1 helix, the linker, and the C-terminal helix are relatively tolerant to mutation.

The mechanosusceptibility of Ec-MscL seems to be the evolutionary purpose of Ec-MscL and not just an evolutionary byproduct. MscL has a specific gating tension that can be increased or decreased by mutation. Additionally for MscL, our data show that it is easier to design mechanosensitivity out of the channel than to design mechanosensitivity into the channel.

4.5 Experimental Procedures

4.5.1 Plasmids and Strains

The Ec-MscL protein was encoded under the control of an IPTG inducible promoter in pB10b, as previously described. All experiments were carried out in the MJF465 bacterial strain that is lacking the MscL, MscS (YggB), and KefA genes.

4.5.2 Random Mutagenesis

Random Mutagenesis of Ec-MscL was performed using the Diversify PCR Random Mutagenesis Kit (CLONTECH) under buffer condition six. A standard PCR reaction using TITANIUM *Taq* DNA polymerase was carried out in the presence of 640 μM $MnSO_4$ and 80 μM dGTP. Following PCR, the reaction products were subcloned into fresh pB10b vector using the Bgl II and Xho I restriction sites.

4.5.3 Phenotypical Characterization of MscL Mutations

Phenotypical characterization of Ec-MscL mutations was carried out as previously described with slight modification to allow growth in deep 96-well plates. Single colonies resulting from the subcloned random Ec-MscL mutations were grown in a 2 mL 96-well growth block using 200 μL of LB medium supplemented with ampicillin (100 μg/mL) for fourteen hours at 37˚C in a shaking incubator (400 RPM). To prevent evaporation and allow gas exchange, the plate was covered with two sheets of 0.5 mil polyester. The LB culture (1 μL) was then used to induce a 200 μL culture in HOEM media supplemented with ampicillin (100 μg/mL) and IPTG (1 mM). The cultures were covered with polyester and grown for seven hours and forty-five minutes at 37˚C in a shaking incubator (400 RPM). In a 96-well plate the HOEM cultures (10 µL) were diluted twentyfold by addition of solutions (190 µL) of various osmotic strengths containing propidium iodide and SYTO 9 (Molecular Probes). Each HOEM culture was subjected to eight different downshock solutions. The downshock solutions were prepared by mixing HOEM media with water in the following ratios; 1:0, 4:1, 13:7, 1:1,

3:5, 1:3, 1:7, and 0:1. After mixing, the 96-well plate was incubated at 37°C in a plate incubator for ninety minutes. The plates were then read using a Gemini XS plate reader (Molecular Devices) with an excitation wavelength of 485 nm and emission wavelengths of 530 nm and 630 nm. Phenotypes were determined from the resulting downshock curves as previously described.

4.5.4 DNA Sequencing

For DNA sequencing, the remaining LB cultures were diluted with TB medium supplemented with ampicillin (100 μg/mL) and grown to saturation. Mini-prep DNA was obtained for sequencing using either a spin mini-prep kit (Qiagen), a 96-well mini-prep kit (Millipore), or using a mini-prep robot (Laragen, Inc., Los Angeles, CA or ACGT, Inc., Northbrook, IL). Big dye terminated automated DNA sequencing (ABI) was performed by either the Caltech Sequence Analysis Facility (Pasadena, CA), Laragen, Inc. (Los Angeles, CA), or ACGT, Inc. (Northbrook, IL).

4.6 Literature Cited

Ajouz, B., Berrier, C., Besnard, M., Martinac, B., and Ghazi, A. (2000). Contributions of the different extramembranous domains of the mechanosensitive ion channel MscL to its response to membrane tension. Journal of Biological Chemistry *275*, 1015-1022.

Blount, P., and Moe, P. C. (1999). Bacterial mechanosensitive channels: integrating physiology, structure and function. Trends in Microbiology *7*, 420-424.

Blount, P., Schroeder, M. J., and Kung, C. (1997). Mutations in a bacterial mechanosensitive channel change the cellular response to osmotic stress. Journal of Biological Chemistry *272*, 32150-32157.

Blount, P., Sukharev, S. I., Schroeder, M. J., Nagle, S. K., and Kung, C. (1996). Single residue substitutions that change the gating properties of a mechanosensitive channel in

Escherichia coli. Proceedings of the National Academy of Sciences of the United States of America *93*, 11652-11657.

Bright-Gaertner, E., and Proulx, P. (1972). MEtabolism of phosphoclycerides in Escherichia coli during growth at 37˚C and during a cold-induced lag phase. Biochimica Et Biophysica Acta *270*, 40-49.

Chang, G., Spencer, R. H., Lee, A. T., Barclay, M. T., and Rees, D. C. (1998). Structure of the MscL homolog from *Mycobacterium tuberculosis*: A gated mechanosensitive ion channel. Science *282*, 2220-2226.

Cruickshank, C. C., Minchin, R. F., LeDain, A. C., and Martinac, B. (1997). Estimation of the pore size of the large-conductance mechanosensitive ion channel of *Escherichia coli*. Biophysical Journal *73*, 1925-1931.

Doyle, D. A., Cabral, J. M., Pfuetzner, R. A., Kuo, A. L., Gulbis, J. M., Cohen, S. L., Chait, B. T., and MacKinnon, R. (1998). The structure of the potassium channel: Molecular basis of K+ conduction and selectivity. Science *280*, 69-77.

Elmore, D. E., and Dougherty, D. A. (2001). Molecular dynamics simulations of wild-type and mutant forms of the *Mycobacterium tuberculosis* MscL channel. Biophysical Journal *81*, 1345-1359.

Elmore, D. E., and Dougherty, D. A. (2002). Investigating mechanosensitive channel of large conductance (MscL) protein-lipid interactions with molecular dynamics simulations. Biophysical Journal *82*, 628A-628A.

Gu, C. X., Juranka, P. F., and Morris, C. E. (2001). Stretch-activation and stretch-inactivation of Shaker-IR, a voltage-gated K+ channel. Biophysical Journal *80*, 2678-2693.

Gu, L. Q., Liu, W. H., and Martinac, B. (1998). Electromechanical coupling model of gating the large mechanosensitive ion channel (MscL) of *Escherichia coli* by mechanical force. Biophysical Journal *74*, 2889-2902.

Gullingsrud, J., Kosztin, D., and Schulten, K. (2001). Structural determinants of MscL gating studied by molecular dynamics simulations. Biophysical Journal *80*, 2074-2081.

Hamill, O. P., and Martinac, B. (2001). Molecular basis of mechanotransduction in living cells. Physiol Rev *81*, 685-740.

Hase, C. C., LeDain, A. C., and Martinac, B. (1997). Molecular dissection of the large mechanosensitive ion channel (MscL) of *E. coli*: Mutants with altered channel gating and pressure sensitivity. Journal of Membrane Biology *157*, 17-25.

Jiang, Y. X., Lee, A., Chen, J. Y., Cadene, M., Chait, B. T., and MacKinnon, R. (2002). Crystal structure and mechanism of a calcium-gated potassium channel. Nature *417*, 515-522.

Jones, S. E., Naik, R. R., and Stone, M. O. (2000). Use of small fluorescent molecules to monitor channel activity. Biochemical and Biophysical Research Communications *279*, 208-212.

Kloda, A., and Martinac, B. (2001). Mechanosensitive channels in Archaea. Cell Biochemistry and Biophysics *34*, 349-381.

Kong, Y. F., Shen, Y. F., Warth, T. E., and Ma, J. P. (2002). Conformational pathways in the gating of *Escherichia coli* mechanosensitive channel. Proceedings of the National Academy of Sciences of the United States of America *99*, 5999-6004.

Lee, R. E., Brennan, P. J., and S., B. G. (1996). *Mycobacterium tuberculosis* cell envelope. Current Topics in Microbiology *215*, 1-27.

Lugtenberg, E. J. J., and Peters, R. (1976). Distribution of lipids in cytoplasmic and outer membranes of Escherichia Coli K12. Biochimica Et Biophysica Acta *441*, 38-47.

Martinac, B., and Hamill, O. P. (2002). Gramicidin A channels switch between stretch activation and stretch inactivation depending on bilayer thickness. Proceedings of the National Academy of Sciences of the United States of America *99*, 4308-4312.

Maurer, J. A., and Dougherty, D. A. (2001). A high-throughput screen for MscL channel activity and mutational phenotyping. Biochimica Et Biophysica Acta-Biomembranes *1514*, 165-169.

Maurer, J. A., Elmore, D. E., Lester, H. A., and Dougherty, D. A. (2000). Comparing and contrasting *Escherichia coli* and *Mycobacterium tuberculosis* mechanosensitive channels (MscL) - New gain of function mutations in the loop region. Journal of Biological Chemistry *275*, 22238-22244.

Okada, K., Moe, P. C., and Blount, P. (2002). Functional design of bacterial mechanosensitive channels: comparisons and contrasts illuminated by random mutagenesis. J Biol Chem *in press*.

Ou, X. R., Blount, P., Hoffman, R. J., and Kung, C. (1998). One face of a transmembrane helix is crucial in mechanosensitive channel gating. Proceedings of the National Academy of Sciences of the United States of America *95*, 11471-11475.

Perozo, E., Cortes, D. M., Sompornpisut, P., Kloda, A., and Martinac, B. (2002a). Open channel structure of MscL and the gating mechanism of mechanosensitive channels. Nature *418*, 942-948.

Perozo, E., Kloda, A., Cortes, D. M., and Martinac, B. (2002b). Physical principles underlying the transduction of bilayer deformation forces during mechanosensitive channel gating. Nature Structural Biology *9*, 696-703.

Rao, J. K. M. (1986). New scoring matrix for amino acid residue exhanges based on residue characteristic physical parameters. International Journal of Peptide and Protein Research *29*, 276-281.

Sukharev, S., Betanzos, M., Chiang, C. S., and Guy, H. R. (2001a). The gating mechanism of the large mechanosensitive channel MscL. Nature *409*, 720-724.

Sukharev, S., Durell, S. R., and Guy, H. R. (2001b). Structural models of the MscL gating mechanism. Biophysical Journal *81*, 917-936.

Sukharev, S. I., Blount, P., Martinac, B., Blattner, F. R., and Kung, C. (1994). A Large-Conductance Mechanosensitive Channel in *E. coli* Encoded by Mscl Alone. Nature *368*, 265-268.

Sukharev, S. I., Blount, P., Martinac, B., and Kung, C. (1997). Mechanosensitive channels of *Escherichia coli*: The MscL gene, protein, and activities. Annual Review of Physiology *59*, 633-657.

Sukharev, S. I., Sigurdson, W. J., Kung, C., and Sachs, F. (1999). Energetic and spatial parameters for gating of the bacterial large conductance mechanosensitive channel, MscL. Journal of General Physiology *113*, 525-539.

Suutari, M., and Laakso, S. (1993). Effects of growth temperature on the fatty acid composition of *Mycobacterium phlei*. Archives of Microbiology *159*, 119-123.

Suutari, M., and Laakso, S. (1994). Microbial fatty acids and thermal adaptation. Critical Reviews in Microbiology *20*, 285-328.

Tabarean, I. V., and Morris, C. E. (2002). Membrane stretch accelerates activation and slow inactivation in Shaker channels with S3-S4 linker deletions. Biophysical Journal *82*, 2982-2994.

Wood, J. M. (1999). Osmosensing by bacteria: Signals and membrane-based sensors. Microbiol Mol Biol Rev *63*, 230.

Yoshimura, K., Batiza, A., Schroeder, M., Blount, P., and Kung, C. (1999). Hydrophilicity of a single residue within MscL correlates with increased channel mechanosensitivity. Biophysical Journal *77*, 1960-1972.

Zhou, Y. F., Morais-Cabral, J. H., Kaufman, A., and MacKinnon, R. (2001). Chemistry of ion coordination and hydration revealed by a K+ channel-Fab complex at 2.0 angstrom resolution. Nature *414*, 43-48.